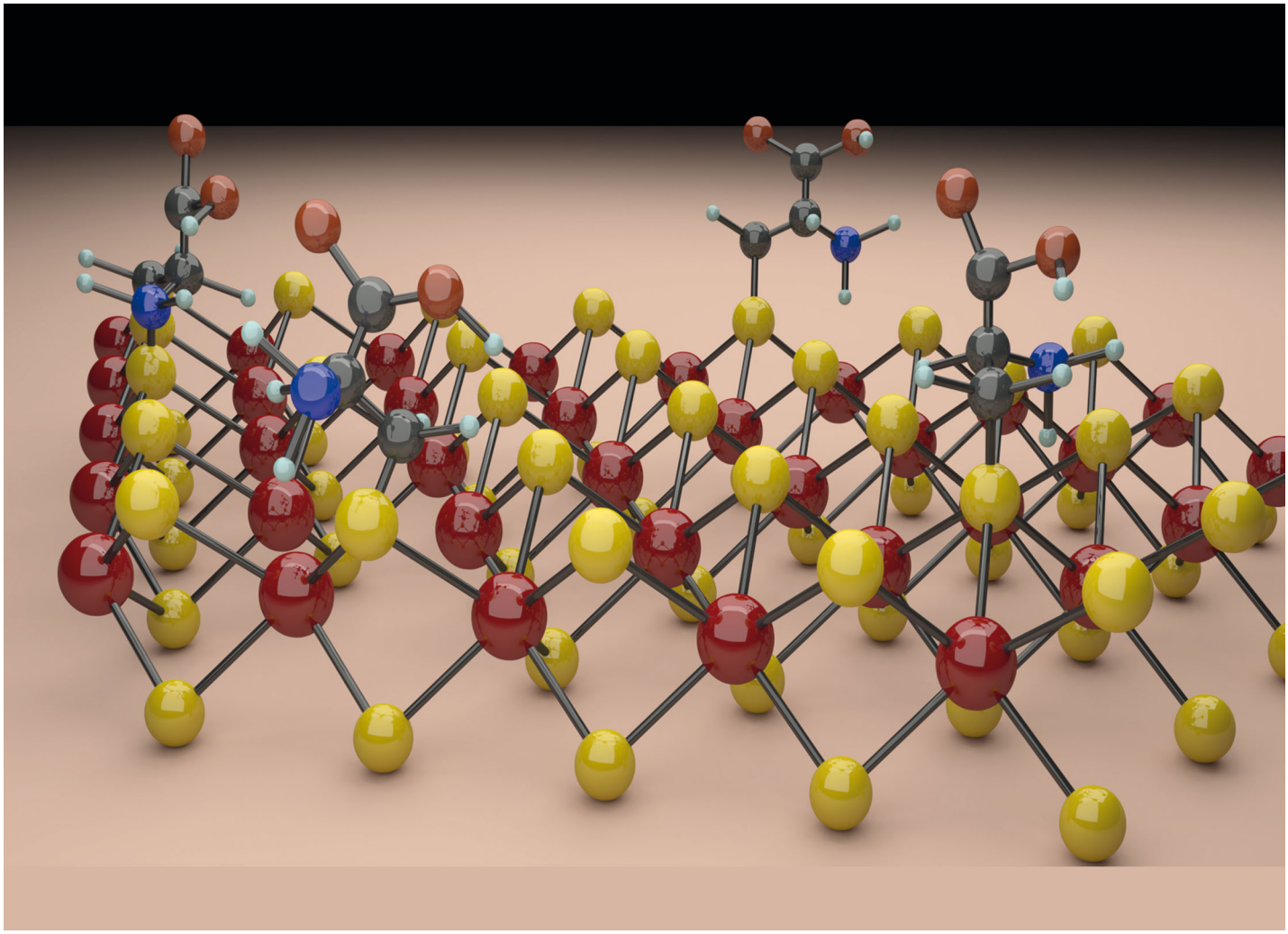

Showcasing research from Professor Rudolf's laboratory, Surfaces and Thin Film Research Group, Zernike Institute for Advanced Materials, University of Groningen, Groningen, The Netherlands.

Photoemission spectroscopy study of structural defects in molybdenum disulfide (MoS_2) grown by chemical vapor deposition (CVD)

The fingerprint of structural defects in CVD grown MoS_2 was revealed by means of X-ray Photoelectron Spectroscopy (XPS). Back cover designed by Ali Syari'ati and Dina Maniar. The Surfaces and Thin Films department of the Zernike Institute for Advanced Materials carries out research on the preparation and analysis of crystalline organic thin films, 2D solids, functional molecules as well as molecular motors and switches on surfaces, and nanocomposites.

As featured in:

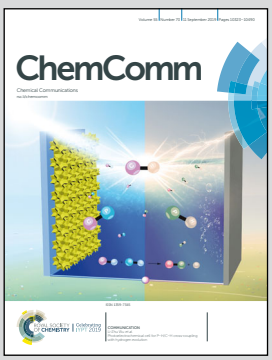

See Petra Rudolf *et al.*, *Chem. Commun.*, 2019, **55**, 10384.

ROYAL SOCIETY OF CHEMISTRY | Celebrating IYPT 2019

rsc.li/chemcomm

Registered charity number: 207890

ChemComm

COMMUNICATION

View Article Online
View Journal | View Issue

Cite this: *Chem. Commun.*, 2019, 55, 10384

Received 25th February 2019,
Accepted 2nd August 2019

DOI: 10.1039/c9cc01577a

rsc.li/chemcomm

Photoemission spectroscopy study of structural defects in molybdenum disulfide (MoS_2) grown by chemical vapor deposition (CVD)†

Ali Syari'ati, Sumit Kumar, Amara Zahid, Abdurrahman Ali El Yumin, Jianting Ye and Petra Rudolf *

The fingerprint of structural defects in CVD grown MoS_2 was revealed by means of X-ray Photoelectron Spectroscopy (XPS). These defects can be partially healed by grafting thiol-functionalized molecules. The functionalization does not alter the semiconducting properties of MoS_2 as confirmed by the photoluminescence spectra.

The extraordinary properties of graphene have sparked increasing interest in other layered materials like Transition Metal Dichalcogenides (TMDCs). TMDCs consist of layers held together by van der Waals (vdW) interaction like graphene layers but here one layer comprises a transition metal atom sheet sandwiched between two chalcogen atom sheets *via* covalent bonds. The weak vdW interaction between the layers can be exploited to isolate two-dimensional (2D) flakes by mechanical,[1,2] chemical[3] and liquid exfoliation,[4–6] but these ultrathin crystals can also be synthesized on suitable substrates by Chemical Vapor Deposition (CVD)[7–10] or Molecular Beam Epitaxy (MBE).[11] MoS_2 has received special attention among TMDCs because its electronic and optoelectronic properties promise well for application in transistors,[2,12,13] sensors,[14] and as a catalyst.[15,16] CVD is the only upscalable method that allows obtaining large domains of single crystalline MoS_2 with sizes reaching hundreds of μm and an electron mobility which approaches that of exfoliated MoS_2.[17] However, so far defects seem unavoidable in CVD grown and exfoliated MoS_2,[18] and can be exploited as catalytic sites for *e.g.* hydrogen evolution reactions.[19] On the other hand, these defects decrease the mobility and photoluminescence (PL) intensity of MoS_2[20–22] and strategies to heal them need to be developed. Zhou *et al.* reported the direct observation by scanning tunneling microscopy of intrinsic structural defects in CVD grown MoS_2,[23] namely sulfur and molybdenum vacancies. Sulfur vacancies can be filled by adsorption of thiol molecules[24] and this strategy can also serve to tune the properties of MoS_2 crystals by functional groups attached to the thiol moiety.[25–27]

In this communication, we monitor structural defects in CVD grown MoS_2 by means of X-ray Photoelectron Spectroscopy (XPS). We demonstrate that the defect density can be increased by thermal annealing, introducing also another type of structural defect. We prove that thiol-terminated cysteine molecules can partially heal the defects by covalently binding to MoS_2 as depicted in Scheme 1. This result differs from the findings of Chen *et al.*, who reported that cysteine molecules merely physisorb on the surface.[28]

MoS_2 crystalline flakes were grown by CVD on oxide-passivated Si wafers (Prime Wafers) as explained in the ESI,† where we detail our reproducible approach to obtain large domain single layer MoS_2.[29] Optical microscopy images showed MoS_2 crystal sizes varying from several to hundreds of μm (see the ESI†). Atomic Force Microscopy and Raman spectroscopy confirmed that MoS_2 (see the ESI†) consists of a single layer. XPS spectra (for experimental details see the ESI†) of the freshly grown sample were collected to minimize contamination from air; 2–4 spots were analysed on each sample to confirm homogeneity. The XPS signal due to adventitious carbon located at 284.8 eV was used as a binding energy (BE) reference.

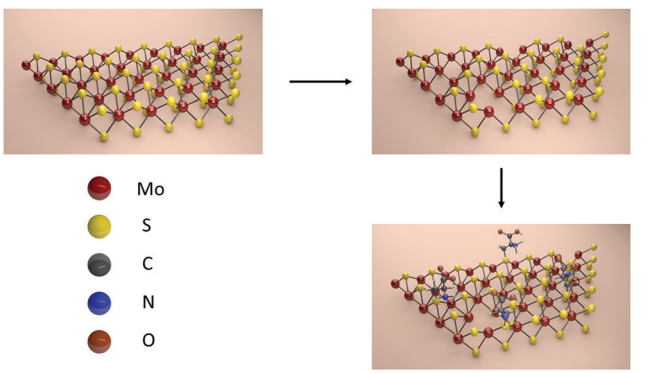

Scheme 1 Functionalization of MoS_2 with cysteine molecules *via* first creating defects through thermal annealing and then filling them with thiol-terminated cysteine.

Zernike Institute for Advanced Materials, University of Groningen, Nijenborgh 4, 9747 AG Groningen, The Netherlands. E-mail: p.rudolf@rug.nl

† Electronic supplementary information (ESI) available. See DOI: 10.1039/c9cc01577a

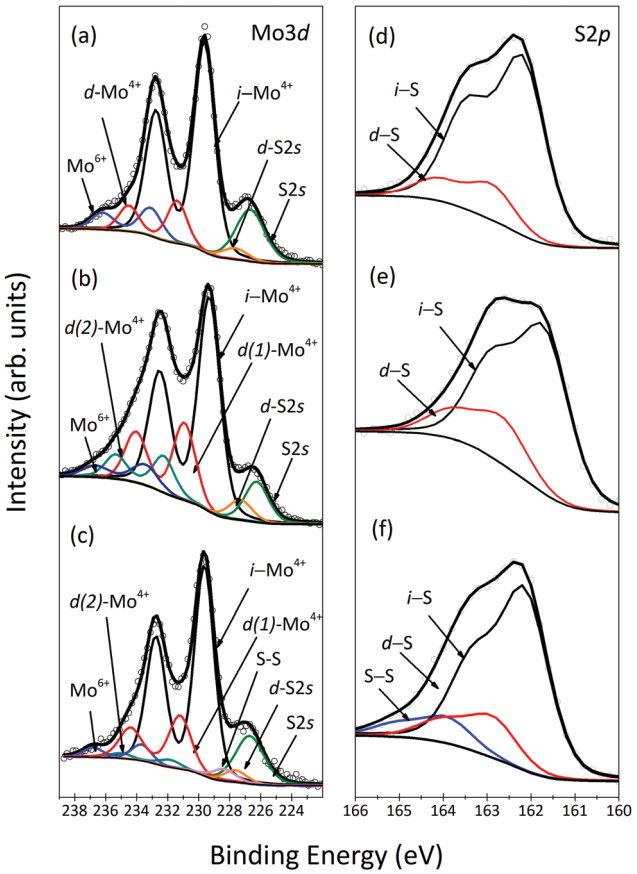

Fig. 1 XPS spectra: Mo3d and S2p core level regions of MoS_2 as-grown (a and d), annealed before (b and e) and after functionalization (c and f).

The spectral region shown in Fig. 1(a) contains both the Mo3d and the S2s core level signals and can be fitted with three Mo3d doublets and two singlet peaks (S2s). The most intense doublet peak, located at a BE of 229.6 eV, is attributed to Mo^{4+} (i-Mo^{4+}), the charge state of molybdenum in MoS_2. The doublet peak located at 1.7 eV higher BE stems from defect Mo^{4+} (d-Mo^{4+}), *i.e.* corresponding to Mo atoms close to sulfur vacancies (V_S).[30,31] Finally, the doublet peak at 233.0 eV BE is due to Mo^{6+} of the unreacted precursor MoO_3,[32] which is always found as a contaminant on CVD grown MoS_2. The most intense singlet peak is due to the S2s emission from defect-free regions of MoS_2, while the additional singlet peak at 227.6 eV corresponds to sulfur close to a defect. The sulfur chemical environment can be more clearly studied by means of the S2p core level spectrum, shown in Fig. 1(d), where two doublets, peaked at 162.4 eV and 163.1 eV, respectively, are observed. We attribute the most intense contribution to intrinsic S (i-S) and the higher BE doublet to sulfur near S vacancies (d-S). This observation is very important because it constitutes the spectroscopic proof of the presence of unsaturated Mo atoms in CVD-grown MoS_2, already observed microscopically by Zhou *et al.*[23]

Thermal annealing is known to induce desorption of S atoms from the MoS_2 nanosheet.[33] Fig. 1(b) shows the XPS spectrum of the Mo3d core level region of the annealed sample, which, apart from a small chemical shift due to band bending,[33] clearly presents a different line shape than the as-grown sample and requires an additional Mo component in the fit. We attribute this new doublet peaked at 231.6 eV (d(2)-Mo^{4+}) to unsaturated Mo atoms close to a more complex defect present in the MoS_2 crystal. We observe a decrease in Mo and S spectral intensity as well as in the S and Mo intensity ratio after annealing. The calculation of the formation energy of the various defects in MoS_2,[31] namely of a molybdenum vacancy (V_{Mo}) and divacancies implying either a missing MoS moiety (V_{MoS}) or two missing sulfur atoms (V_{SS}), gives the lowest value for V_{Mo}, and only a 0.2 eV higher value for V_{MoS} and V_{SS}, making it difficult to discriminate which defects are formed after annealing. Since d(2)-Mo^{4+} appears at a higher BE than d(1)-Mo^{4+} and i-Mo^{4+} we can conclude that it is associated with the loss of S atoms; in fact more than one missing S implies even more positive charge on the surrounding Mo atoms.[31] After annealing, we also observe a 10 ± 2% intensity increase of the component attributed to d(1)-Mo^{4+}, confirming the assignment to V_S in the MoS_2 nanosheet; moreover the d(1)-Mo^{4+} component is shifted to lower BE, confirming additional loss of S in the surroundings of V_s.[34]

The desorption of S atoms is also observed in the S2p spectrum of the annealed sample, depicted in Fig. 1(e), where the intensity of the component assigned to the d-S peak increased by 11%. The rigid binding energy shift was also observed for S2p spectral lines upon annealing, similar to the result reported by Donarelli *et al.*[33]

To explore whether these structural defects can be healed by thiol-functionalized molecules, we exposed MoS_2 to thiol-terminated cysteine. Functionalization of freshly grown MoS_2 resulted in a barely noticeable change in the XPS spectra due to undesired contamination blocking adsorption sites (see the ESI†). The XPS spectra of the Mo3d and the S2s core level region and the S2p core level region of functionalized annealed MoS_2 are shown in Fig. 1(c) and (f), respectively. In the spectrum of Fig. 1(c), one notes that the exposure to thiol-functionalized cysteine induced a 3 ± 2% decrease in the d(1)-Mo^{4+} spectral intensity and a 8 ± 2% decrease in the d(2)-Mo^{4+} spectral intensity. Chu *et al.* reported that monosulfur vacancies can act as the centers for the functionalization because when one thiol molecule is attached it facilitates the adsorption of other molecules to neighbouring vacancies in the range of 9–36 $Å^2$ from the first adsorbate.[35] Interestingly, the two components are also shifted towards higher BE, with the d(2)-Mo^{4+} doublet now peaked at 232.0 eV and the d(1)-Mo^{4+} doublet peaked at 231.2 eV. This observation indicates that the adsorbed molecules not only heal the structural defects but also promote charge transfer, a mechanism, which could be used to tailor the electronic properties of MoS_2. In agreement with a previous discussion of the Mo spectra, upon functionalization (Fig. 1(f)) a noticeable decrease of 10.8% of the intensity of the d-S component was observed, confirming preferential healing of monosulfur vacancies. Furthermore, a new contribution appeared at 164.2 eV, attributed to S–S bonds,[28] corroborating adsorption of a second cysteine molecule close to a first one, which also supports the result of the Mo3d spectra.[36]

Confirmation for the presence of cysteine grafted onto the MoS_2 basal plane also comes from the XPS spectra of the C1s

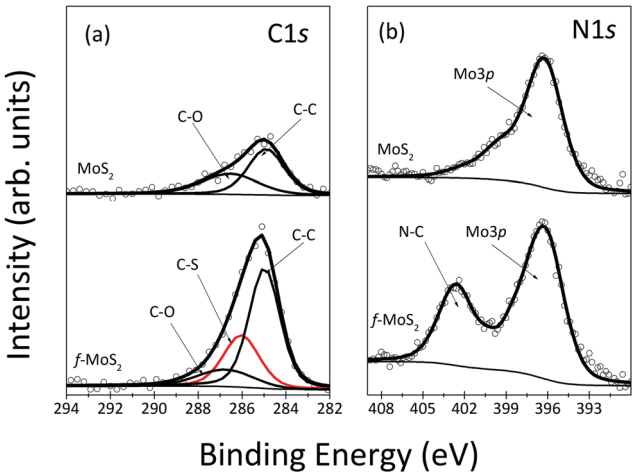

Fig. 2 XPS spectra of C1s (a) and N1s (b) core level regions of as-grown MoS_2 and after functionalization of annealed MoS_2.

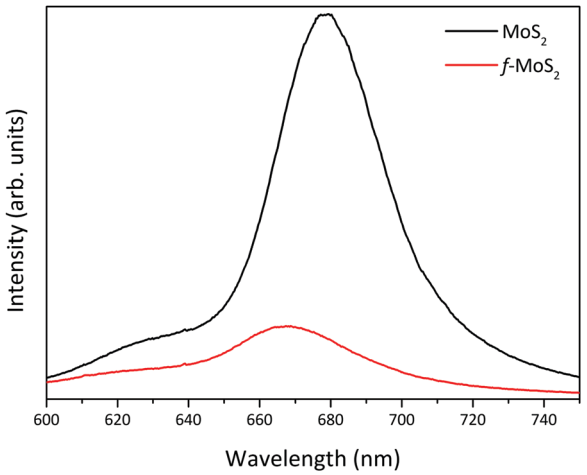

Fig. 4 PL spectra before (MoS_2) and after functionalization (f-MoS_2).

and N1s core level regions of the functionalized MoS_2 shown in Fig. 2. In Fig. 2(a), the adventitious carbon with C–C and C–O bonds was observed in the as-grown sample. Upon functionalization, as expected, the spectral intensity of these components increased, together with the appearance of a new component at 286.0 eV due to C–S bonds; the relative increases in intensity agree with what is expected from the molecular structure of cysteine. In Fig. 2(b), the nitrogen peak observed at 403.4 eV corresponds to the N–C bond, again as expected for adsorbed cysteine.

FTIR spectroscopy is a fast and non-destructive tool to confirm the covalent functionalization of the MoS_2 nanosheet;[28,37,38] therefore, we collected the Attenuated Total Reflection Fourier Transform Infra-Red (ATR-FTIR) spectrum of functionalized MoS_2 to support the XPS data. The spectrum is shown in Fig. 3 together with the spectrum of cysteine for reference. The S–H stretching vibration (ν_{S-H}) at 2549 cm^{-1}, clearly observed in cysteine but absent for functionalized MoS_2, points to H splitting off when the molecules bind to the MoS_2 basal plane.[39] Furthermore, the presence of a band at 700 cm^{-1}, typical of the C–S stretching vibration, can be taken as evidence of the successful functionalization.[40] The presence of this feature in both samples proves the presence of cysteine on MoS_2 and supports the XPS data.

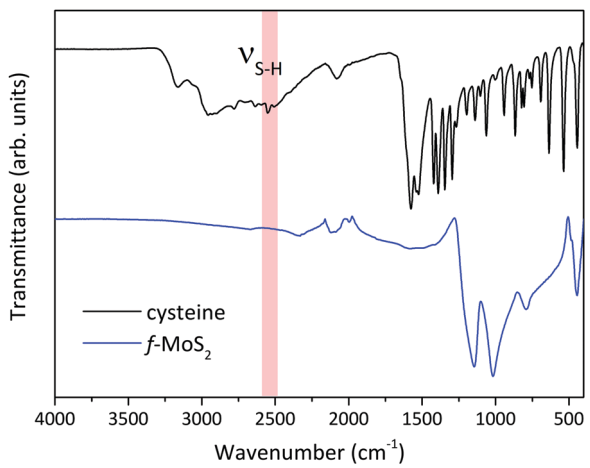

Fig. 3 ATR-FTIR spectra of cysteine and defect-rich MoS_2 after functionalization with thiol-terminated cysteine.

Unlike another covalent functionalization strategy,[41,42] which requires transformation of the semiconducting 2H-MoS_2 phase into metallic MoS_2 (1T-MoS_2), the covalent functionalization performed in this work preserves the semiconducting nature of the TMDC, as demonstrated by the photoluminescence (PL) spectrum in Fig. 4. Upon functionalization, MoS_2 shows a PL peak at 668 nm, which is absent in the case of 1T-MoS_2.[24] However, the PL intensity decreased and the peak is slightly blue-shifted due to the doping from the cysteine molecules, in agreement with the XPS results.

In conclusion, we identified the XPS fingerprint of the structural defects in CVD grown MoS_2 and demonstrated that when thermal annealing causes sulfur to desorb from the basal plane of MoS_2, vacancies with more than one missing sulfur atom are created. Most importantly we proved that partial filling of vacancies is possible *via* covalent functionalization of defective MoS_2 with thiol-terminated cysteine. After functionalization MoS_2 maintains its semiconducting characteristics.

A. Syari'ati thanks the Indonesian Endowment Fund for Education (LPDP) for supporting his PhD study. This work was supported by the Advanced Materials Research Program of the Zernike National Research Centre under the Bonus Incentive Scheme of the Dutch Ministry for Education, Culture and Science.

Conflicts of interest

There are no conflicts to declare.

Notes and references

1 Q. H. Wang, K. Kalantar-Zadeh, A. Kis, J. N. Coleman and M. S. Strano, *Nat. Nanotechnol.*, 2012, **7**, 699–712.
2 Y. Zhang, J. Ye, Y. Matsuhashi and Y. Iwasa, *Nano Lett.*, 2012, **12**, 1136–1140.

3 G. Eda, H. Yamaguchi, D. Voiry, T. Fujita, M. Chen and M. Chhowalla, *Nano Lett.*, 2011, **11**, 5111–5116.
4 J. N. Coleman, M. Lotya, A. O'Neill, S. D. Bergin, P. J. King, U. Khan, K. Young, A. Gaucher, S. De, R. J. Smith, I. V. Shvets, S. K. Arora, G. Stanton, H.-Y. Kim, K. Lee, G. T. Kim, G. S. Duesberg, T. Hallam, J. J. Boland, J. J. Wang, J. F. Donegan, J. C. Grunlan, G. Moriarty, A. Shmeliov, R. J. Nicholls, J. M. Perkins, E. M. Grieveson, K. Theuwissen, D. W. McComb, P. D. Nellist and V. Nicolosi, *Science*, 2011, **331**, 568–571.
5 G. Cunningham, M. Lotya, C. S. Cucinotta, S. Sanvito, S. D. Bergin, R. Menzel, M. S. P. Shaffer and J. N. Coleman, *ACS Nano*, 2012, **6**, 3468–3480.
6 H. B. Sim, J. Y. Lee, B. Park, S. J. Kim, S. Kang, W. H. Ryu and S. C. Jun, *Nano Res.*, 2016, **9**, 1709–1722.
7 J. Jeon, S. K. Jang, S. M. Jeon, G. Yoo, Y. H. Jang, J.-H. Park and S. Lee, *Nanoscale*, 2014, 1–10.
8 Y. Lee, S. Park, H. Kim, G. H. Han, Y. H. Lee and J. Kim, *Nanoscale*, 2015, **7**, 11909–11914.
9 L. Tao, K. Chen, Z. Chen, W. Chen, X. Gui, H. Chen, X. Li and J.-B. Xu, *ACS Appl. Mater. Interfaces*, 2017, **9**, 12073–12081.
10 Y. Kim, H. Bark, G. H. Ryu, Z. Lee and C. Lee, *J. Phys.: Condens. Matter*, 2016, **28**, 6.
11 D. Fu, X. Zhao, Y.-Y. Zhang, L. Li, H. Xu, A.-R. Jang, S. I. Yoon, P. Song, S. M. Poh, T. Ren, Z. Ding, W. Fu, T. J. Shin, H. S. Shin, S. T. Pantelides, W. Zhou and K. P. Loh, *J. Am. Chem. Soc.*, 2017, **139**, 9392–9400.
12 B. Radisavljevic, A. Radenovic, J. Brivio, V. Giacometti and A. Kis, *Nat. Nanotechnol.*, 2011, **6**, 147–150.
13 J. Kang, W. Liu and K. Banerjee, *Appl. Phys. Lett.*, 2014, **104**, 093106.
14 A. Smolyanitsky, B. I. Yakobson, T. A. Wassenaar, E. Paulechka and K. Kroenlein, *ACS Nano*, 2016, **10**, 9009–9016.
15 M. A. Lukowski, A. S. Daniel, F. Meng, A. Forticaux, L. Li and S. Jin, *J. Am. Chem. Soc.*, 2013, **135**, 10274–10277.
16 E. E. Benson, H. Zhang, S. A. Schuman, S. U. Nanayakkara, N. D. Bronstein, S. Ferrere, J. L. Blackburn and E. M. Miller, *J. Am. Chem. Soc.*, 2018, **140**, 441–450.
17 J. Chen, W. Tang, B. Tian, B. Liu, X. Zhao, Y. Liu, T. Ren, W. Liu, D. Geng, H. Y. Jeong, H. S. Shin, W. Zhou and K. P. Loh, *Adv. Sci.*, 2016, **3**, 1500033.
18 J. Hong, Z. Hu, M. Probert, K. Li, D. Lv, X. Yang, L. Gu, N. Mao, Q. Feng, L. Xie, J. Zhang, D. Wu, Z. Zhang, C. Jin, W. Ji, X. Zhang, J. Yuan and Z. Zhang, *Nat. Commun.*, 2015, **6**, 6293.
19 G. Ye, Y. Gong, J. Lin, B. Li, Y. He, S. T. Pantelides, W. Zhou, R. Vajtai and P. M. Ajayan, *Nano Lett.*, 2016, **16**, 1097–1103.
20 H. Nan, Z. Wang, W. Wang, Z. Liang, Y. Lu, Q. Chen, D. He, P. Tan, F. Miao, X. Wang, J. Wang and Z. Ni, *ACS Nano*, 2014, **8**, 5738–5745.
21 W. Su, L. Jin, X. Qu, D. Huo and L. Yang, *Phys. Chem. Chem. Phys.*, 2016, **18**, 14001–14006.
22 Z. Yu, Y. Pan, Y. Shen, Z. Wang, Z.-Y. Ong, T. Xu, R. Xin, L. Pan, B. Wang, L. Sun, J. Wang, G. Zhang, Y. W. Zhang, Y. Shi and X. Wang, *Nat. Commun.*, 2014, **5**, 5290.
23 W. Zhou, X. Zou, S. Najmaei, Z. Liu, Y. Shi, J. Kong, J. Lou, P. M. Ajayan, B. I. Yakobson and J. C. Idrobo, *Nano Lett.*, 2013, **13**, 2615–2622.
24 D. M. Sim, M. Kim, S. Yim, M. J. Choi, J. Choi, S. Yoo and Y. S. Jung, *ACS Nano*, 2015, **9**, 12115–12123.
25 R. Canton-Vitoria, Y. Sayed-Ahmad-Baraza, M. Pelaez-Fernandez, R. Arenal, C. Bittencourt, C. P. Ewels and N. Tagmatarchis, *npj 2D Mater. Appl.*, 2017, **1**, 13.
26 P. Vishnoi, A. Sampath, U. V. Waghmare and C. N. R. Rao, *Chem. – A Eur. J.*, 2017, **23**, 886–895.
27 E. P. Nguyen, B. J. Carey, J. Z. Ou, J. Van Embden, E. Della Gaspera, A. F. Chrimes, M. J. S. Spencer, S. Zhuiykov, K. Kalantar-Zadeh and T. Daeneke, *Adv. Mater.*, 2015, **27**, 6225–6229.
28 X. Chen, N. C. Berner, C. Backes, G. S. Duesberg and A. R. McDonald, *Angew. Chem., Int. Ed.*, 2016, **55**, 5803–5808.
29 A. Syari'ati, A. Ali, E. Yumin, T. Zehra, B. Kooi, J. Ye and P. Rudolf, *unpublished*.
30 I. S. Kim, V. K. Sangwan, D. Jariwala, J. D. Wood, S. Park, K. S. Chen, F. Shi, F. Ruiz-Zepeda, A. Ponce, M. Jose-Yacaman, V. P. Dravid, T. J. Marks, M. C. Hersam and L. J. Lauhon, *ACS Nano*, 2014, **8**, 10551–10558.
31 S. Haldar, H. Vovusha, M. K. Yadav, O. Eriksson and B. Sanyal, *Phys. Rev. B: Condens. Matter Mater. Phys.*, 2015, **92**, 1–12.
32 D. Ganta, S. Sinha and R. T. Haasch, *Surf. Sci. Spectra*, 2014, **21**, 19–27.
33 M. Donarelli, F. Bisti, F. Perrozzi and L. Ottaviano, *Chem. Phys. Lett.*, 2013, **588**, 198–202.
34 M. A. Baker, R. Gilmore, C. Lenardi and W. Gissler, *Appl. Surf. Sci.*, 1999, **150**, 255–262.
35 X. S. Chu, A. Yousaf, D. O. Li, A. A. Tang, A. Debnath, D. Ma, A. A. Green, E. J. G. Santos and Q. H. Wang, *Chem. Mater.*, 2018, **30**, 2112–2128.
36 K. C. Knirsch, N. C. Berner, H. C. Nerl, C. S. Cucinotta, Z. Gholamvand, N. McEvoy, Z. Wang, I. Abramovic, P. Vecera, M. Halik, S. Sanvito, G. S. Duesberg, V. Nicolosi, F. Hauke, A. Hirsch, J. N. Coleman and C. Backes, *ACS Nano*, 2015, **9**, 6018–6030.
37 C. Backes, N. C. Berner, X. Chen, P. Lafargue, P. LaPlace, M. Freeley, G. S. Duesberg, J. N. Coleman and A. R. McDonald, *Angew. Chem., Int. Ed.*, 2015, **54**, 2638–2642.
38 X. Chen and A. R. McDonald, *Adv. Mater.*, 2016, 5738–5746.
39 E. Satheeshkumar, A. Bandyopadhyay, M. B. Sreedhara, S. K. Pati, C. N. R. Rao and M. Yoshimura, *ChemNanoMat*, 2017, **3**, 172–177.
40 S. F. Parker, *Chem. Phys.*, 2013, **424**, 75–79.
41 S. Presolski and M. Pumera, *Mater. Today*, 2016, **19**, 140–145.
42 D. Voiry, A. Goswami, R. Kappera, C. D. C. C. E. Silva, D. Kaplan, T. Fujita, M. Chen, T. Asefa and M. Chhowalla, *Nat. Chem.*, 2015, **7**(1), 45–49.